Boulder-Munich II: Properties of Hot, Luminous Stars
ASP Conference Series, Vol. 131, 1998
Ian D. Howarth (ed.)

Realistic Models for Expanding Atmospheres

A. W. A. Pauldrach, M. Lennon[1], T. L. Hoffmann, F. Sellmaier, R.-P. Kudritzki[1], and J. Puls

Universitätssternwarte München, Scheinerstr. 1, D-81679 München, Germany

Abstract. In this paper we describe the status of the continuing effort to construct realistic models for expanding atmospheres (e.g., radiation driven winds of hot stars, SNIa, and novae). The potential of our theoretical concept is demonstrated by an application to the O3 Iaf star HD 93129A. We present our method of O-star diagnostics, which is based on a comparison of observed spectra with calculated synthetic high-resolution spectra covering the observable UV region. As a result we get physical constraints on the properties of stellar winds, and the stellar parameters and abundances can be determined.

Although such models already reproduce the observed quantities satisfactorily the method is still affected by shortcomings. Special emphasis is therefore given to the latest improvements which involve a fundamental step towards a realistic description of stationary wind models. These improvements comprise the use of accurate atomic data for a very detailed multilevel non-LTE treatment of the metal ions, the revised inclusion of EUV and X-ray radiation by shock-heated matter, and, most importantly, *the consistent calculation of line blocking and blanketing.* With the solution of the latter problem the astrophysically important information about the ionizing fluxes of O stars is obtained as a by-product.

1. Introduction

Detailed spectrum syntheses which fully extract the quantitative information contained in the spectral domains of the EUV, the UV, and the optical, are still one of the main objectives in hot-star physics. In particular, the ultraviolet spectra of hot stars, with their hundreds of spectral lines formed far out in the wind at high outflow velocities (e.g., the resonance lines of the CNO elements; see Fig. 1), as well as in deeper atmospheric layers at velocities comparable to the sound velocity (e.g., the strongly wind contaminated lines mainly of the iron-group elements; see Fig. 1), can provide important information about stellar parameters, wind properties, and abundances. The aim is to determine these quantities via the application of model atmospheres and to calculate stellar

[1]Affiliated to Max-Planck Institut für Astrophysik, Karl-Schwarzschild-Str. 1, D-85740 Garching, Germany

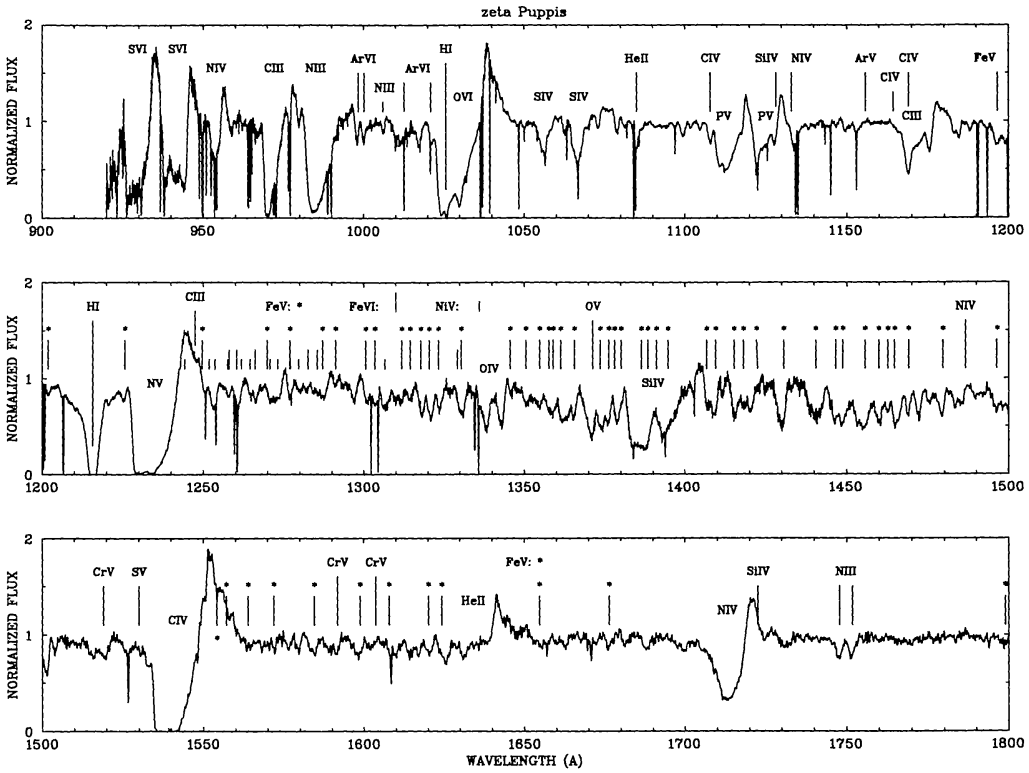

Figure 1. Observed Copernicus (900–1500Å; Morton & Underhill 1977) and IUE (1500–1800Å; Walborn et al. 1985) high-resolution UV spectrum of the O4 I(f) star ζ Puppis. The most important strong and weak winds lines are identified and marked. The large number of wind contaminated Fe V lines between 1250 and 1500Å is striking. (From Pauldrach et al. 1994b.)

energy distributions and, hence, ionizing fluxes which are of further importance in the formation of emission-line spectra of gaseous nebulae (e.g., H II regions and planetary nebulae). However, due to the complexity of the theory of hot-star atmospheres, which requires sophisticated non-LTE calculations and a hydrodynamical treatment that includes the effects of expanding atmospheres, this is a long-standing problem which was only partially – or on the basis of questionable approximations – realized in the past. (A large compilation of references relating to this is given by Kudritzki 1998.) *Realistic models* are now required, by which we mean those which fully reproduce the observed high-resolution spectra of hot stars via consistently calculated synthetic spectra, and which reproduce the energy distribution in the EUV in a detailed and correct way.

Although our theoretical tools are still in an exploratory stage we have already taken first real steps in this direction. So far we have constructed hydrodynamic atmospheric models for seven O stars: the O4 I(f) star ζ Puppis (cf. Pauldrach et al. 1994a) and the O3 If* star HD 93129A (cf. Taresch et al. 1997) in the Galaxy; the O3 If/WN star Mk42 (cf. Pauldrach et al. 1994a), the O3 III(f*) star Sk−68°137, and the O4 If$^+$ star Sk−67°166 in the LMC; and

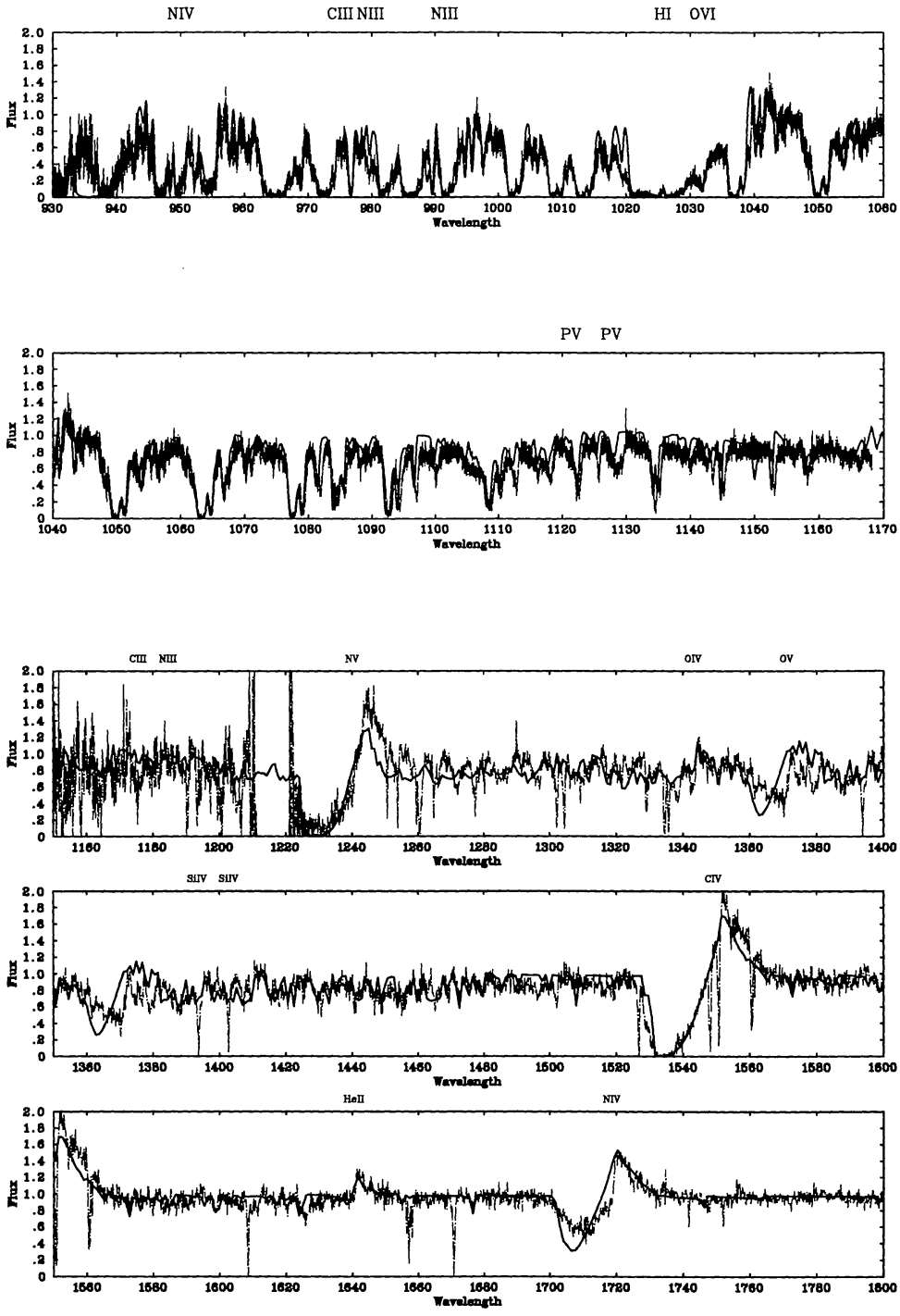

Figure 2. Comparison of observed and calculated synthetic spectrum of the O3 If* star HD 93129A. The upper two panels show the ORFEUS spectrum, where the interstellar molecular lines of H_2 and HD are included in the spectrum fit. The lower three panels show the usual IUE spectrum where the narrow sharp interstellar lines are not included in the spectral fit. (From Taresch et al. 1997).

the O3 III(f*) star NGC 346 No. 3 and the O6 V star AV 243 in the SMC (for the last four objects cf. Haser et al. 1997).

In the analyses, UV spectra (observed with IUE, ORFEUS, and HST), together with some optical lines, have been investigated, where the quantitative spectroscopic studies, based on our non-LTE hydrodynamic model atmosphere code described in Pauldrach et al. (1994a, 1994b), resulted in the determination of abundances, $\log g$, and $T_{\rm eff}$. Fig. 2 shows as an example the final fit of the comparison performed for HD 93129A. Although the agreement is quite convincing, and the stellar and wind parameters determined coincide with those obtained from *unified* atmospheric non-LTE analyses of H and He lines in the visual region (cf. Puls et al. 1996, 1998), we still observe deviations for some individual lines (for instance, the subordinate line of O v at 1371Å). Having found from this kind of model calculation that the behaviour of a number of spectral lines is critically dependent on a detailed and consistent description of *line blocking and line blanketing,* we attribute these deviations to the restrictive approximations which we used for this important part of the method. Hence, the next quantitative approach requires a realistic and consistent description of line blocking and blanketing. In Section 3 we will present a method which fulfills these requirements and, in connection, we will report on problems we have been faced with in calculating the ionizing fluxes of O stars correctly. As a basis for this discussion the general concept and the status of our treatment of hydrodynamic expanding atmospheres is summarized in Section 2.

2. The Concept of Radiation Driven Winds

The concept of our expanding-atmosphere model calculations is based on the homogeneous, stationary, and spherically symmetric radiation-driven wind theory initially outlined by Lucy & Solomon (1970) and Castor, Abbott & Klein (1975). This concept turned out to be adequate for the analyses of hot-star spectra (see Fig. 2) and in spite of its restrictive character we are confident that in general it correctly describes the time-average mean of the spectral features. Fig. 3 gives an overview of the physics to be treated, and in the following we will briefly discuss the characteristic features of the system and describe our model approach. (A comprehensive discussion of most points is found in Pauldrach et al. 1994a.)

The principal features are:

- *The hydrodynamic equations* are solved for pre-specified values of the stellar parameters $T_{\rm eff}$, $\log g$, R_*, and Z (abundances). The crucial term is the radiative acceleration $g_{\rm rad}$, which has contributions from continuous absorption, scattering, and line absorption (the last term is calculated by summing the contributions of lines selected from our list containing more than 2 500 000 lines).

- *The occupation numbers* for up to 5000 levels are determined by the *rate equations* containing collisional (C_{ij}) and radiative (R_{ij}) transition rates. For the calculation of the radiative bound-bound transition probabilities the Sobolev plus continuum method is used (cf. Hummer & Rybicki 1985,

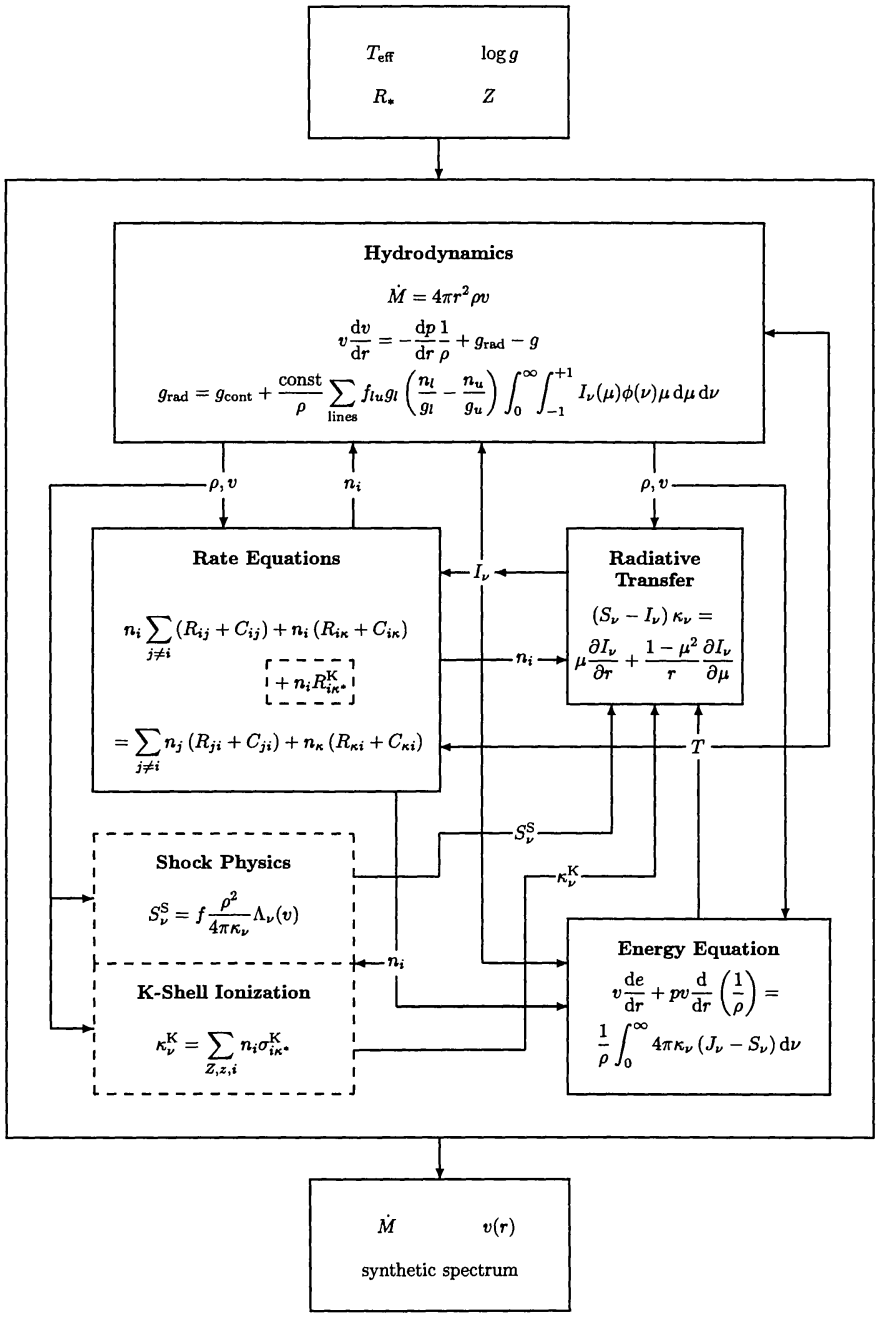

Figure 3. Schematic sketch of the basic equations of stationary radiation-driven wind theory (see text).

Puls & Hummer 1988, and Taresch et al. 1997). Low-temperature dielectronic recombination is included (in total 20 000 transitions) and Auger ionization due to K-shell absorption (considered for C, N, O, Ne, Mg, Si, and S) of soft X-ray radiation arising from shock-heated matter is taken into account.

- *The spherical-transfer equation* which yields the radiation field in the observer's frame at up to 3500 frequency points at every depth point, including the thermalized layers where the diffusion approximation is applied, is correctly solved for the total opacities (κ_ν) and source functions (S_ν). Hence, the strong EUV *line blocking,* which acts mainly between 228Å and 911Å and which constitutes the ionizing flux and influences the ionization and excitation of levels, is properly taken into account (see Section 3).

  Moreover, the emission from *shocks* arising from the non-stationary, unstable behaviour of radiation-driven winds (see, for instance, Prinja & Howarth 1986) is, together with K-shell absorption, also included in the radiative transfer. For the calculation of the *shock source function* ($S_\nu^{\rm S}$) we did not directly use the results of the theoretical investigation of time-dependent radiation hydrodynamics that describes the creation and development of shocks (cf. Owocki, Castor & Rybicki 1988; Feldmeier 1995, 1998; note that the reliability of these calculations was recently demonstrated by a comparison to ROSAT observations (cf. Feldmeier et al. 1997)). Instead, the shock source function was incorporated in a preliminary way on the basis of an approximate calculation where the volume emission coefficient (Λ_ν) of the X-ray plasma is calculated using the Raymond & Smith (1977) code (cf. Hunsinger 1993) and the velocity-dependent post-shock temperatures and the filling factor (f) enter as fit parameters (cf. Pauldrach et al. 1994b).

- *The temperature structure* is determined by the microscopic *energy equation* which, in principle, states that the luminosity must be conserved. In our present calculations *line blanketing* effects which reflect the influence of line blocking on the temperature structure are taken into account (see Section 3).

- The iterative solution of the total system of equations then yields the hydrodynamic structure of the wind (i.e., the *mass-loss rate* [$\dot{M}$] and the *velocity structure* [$v(r)$]) together with *synthetic spectra* and ionizing fluxes.

As our present treatment of O-star atmospheric models is of course not free from approximations – in common with all other approaches to the theory (e.g., Schaerer & de Koter 1997; Hillier & Miller 1997) – we will emphasize the crucial points which either have important consequences or which still imply some uncertainties for our model calculations in more detail.

2.1. Atomic Models

It is obvious that detailed non-LTE spectrum-synthesis calculations require accurate atomic data, since the quality of the synthetic spectra cannot be better than the quality of the input data. Hence, we have to improve the basis of

our work – the atomic models – continuously. At present we have replaced the atomic models of the most important ions of the 149 ionization stages of 26 elements considered in order to improve the quality. Eighty per cent of these improvements were implemented by utilizing the SUPERSTRUCTURE program

Table 1. Summary of Atomic Data. Columns 2 and 3 give the number of levels in packed and unpacked form; in columns 4 and 5 are given the number of lines used in the rate equations and for the line-force & blocking calculations, respectively.

Ion	Number of packed levels	Number of levels	Total non-LTE lines	Total lines
C III	50	90	520	4407
C IV	27	48	103	229
N III	40	80	356	16458
N IV	50	90	520	4201
N V	27	47	104	229
O III	50	118	582	25511
O IV	44	90	435	17933
O V	50	88	524	4336
Ne III	38	78	319	857
Ne IV	50	113	577	4470
Ne V	50	110	534	2664
Si III	50	88	480	4044
Si IV	25	45	90	245
Si VI	50	122	596	3889
S III	14	28	32	190
S IV	13	23	22	70
S V	14	26	17	82
S VI	18	32	59	142
Ar III	13	26	21	1912
Ar IV	11	23	22	398
Ar V	40	96	328	3007
Ar VI	42	93	400	1335
Fe III	50	122	246	199484
Fe IV	45	126	253	14346
Fe V	50	122	442	10831
Fe VI	50	104	452	11533
Ni III	40	112	281	131508
Ni IV	50	148	528	11979
Ni V	41	95	70	9207
Ni VI	45	128	253	10821

(Eissner et al. 1974, Nussbaumer & Storey 1978), which uses the configuration-interaction approximation to determine wave functions and radiative data. The remaining part of the data was taken from the Kurucz (1992) line list and from the Opacity Project (cf. Seaton et al. 1994; Cunto & Mendoza 1992); the latter was also a source for photoionization cross-sections. Collisional data have largely become available through the IRON project (see Hummer et al. 1993). Table 1 gives an overview of the affected ions.

3. Non-LTE Line Blocking and Blanketing

From the discussion in the previous sections it is evident that the construction of realistic models for expanding atmospheres requires a correct and consistent description of line blocking and blanketing. The method for this is well established for cold stars, where the atmospheres are hydrostatic and the assumption of LTE is justified (cf. Kurucz 1979, 1992); the method fails, however, for hot stars, where non-LTE effects are prominent and the atmospheres are expanding rapidly. In this case one has to account for:

(i) The *line shift* caused by the Doppler effect due to the velocity field.

(ii) The influence of line blocking on the radiative photoionization rates.

(iii) The correct influence of the line-blocked radiation field on the radiative bound-bound rates.

(iv) The correct incident radiation for the radiative acceleration term.

(v) The influence of line blocking opacities on the energy balance.

The first three items are connected to the fact that the radiation field is drastically reduced in the EUV due to line opacities and is redistributed to lower energies. The important effect of the velocity field thereby is that it increases the frequency range which can be blocked by a single line. The fourth item reflects what is usually meant by *line overlap* (see, for instance, Puls 1987), and the last item concerns the increase of the Rosseland optical depth and in consequence of the temperature due to line opacities; this refers to *line blanketing.*

So far, there are two other approaches to the theory which try to overcome the problem as described above. The method presented by Schaerer & Schmutz (1994; see also Schaerer & de Koter 1997) is at present restricted, since they do not solve the rate equations for the metals (most importantly, non-LTE calculations for Fe are missing) and hence they cannot account for items (ii) and (iii), whereas the method by Hillier & Miller (1997) does not appear to have basic restrictions. In the following we will give an overview of our approach.

3.1. The Treatment of Line Blocking

The approach which is best suited for our purposes is the *opacity sampling* technique (cf. Peytremann 1974; Sneden et al. 1976). This method allows us to account for the *line shift* in the wind, since a rearrangement of opacities, as required for opacity distribution functions (cf. Hubeny et al. 1998), does not

take place. In this way, the correct influence of line blocking on bound-bound transitions (cf. item (iii)), which has to conserve the frequential position, can be treated.

For the *opacity sampling,* a set of frequency points is distributed in a logarithmic scale over the relevant spectral range (~160Å–1200Å for O stars) and the transfer equation is solved for each point. Note that for the ionization calculations it is important to extend the line-blocking calculations to the range shortward of the He II edge (cf. Pauldrach et al. 1994a).

In this way the exact solution is reached by increasing the number of frequency points. By investigating the accuracy of typical photoionization integrals we found that convergence can be achieved with approximately 1000 to 2000 frequency points in the relevant range (cf. Sellmaier 1996; Pauldrach et al. 1997). The advantages of the opacity sampling method are obvious: we can investigate the effects of line blocking on selected bound-bound transitions if we spread additional points around the transition frequency of interest; furthermore, we can apply the Doppler shift to the line absorption and emission coefficients.

3.2. The Treatment of the Line Shift.

The line opacity at a certain sampling frequency ν is the sum over all (integrated) line opacities $\overline{\chi}_l$ multiplied by the line profile function $\varphi_l(\nu)$:

$$\chi_{lb}(\nu) = \sum_{\text{lines}} \overline{\chi}_l \varphi_l(\nu). \tag{1}$$

In the static part of the atmosphere a line covers with its Doppler profile (φ_D) only a small frequency range around the transition frequency ν_0 (illustrated in Fig. 4 on the right-hand side; note that with respect to our sampling grid, 40 per cent of the available lines are treated in the static part).

In the expanding part of the atmosphere the line shift due to the velocity field, $\nu = \nu_0(1 + v(r)/c)$, is applied to the individual line opacities before the summation in Eqn. 1 is carried out at each sampling and depth point. However, from the upper panel of Fig. 4 it is obvious that if the line opacity is simply shifted along the comoving frame frequency (ν_{CMF}) to every radius point successively, many frequency points miss the line, since the radius grid is too coarse to treat large line shifts in the observer's frame. This behaviour is corrected by assuming a boxcar profile $\varphi_{\Delta v}$ representing the velocity range around each radius point (see Fig. 4, lower panel).

The convolution $(\varphi_D \otimes \varphi_{\Delta v})(\nu)$ results in the final profile function which for $\Delta v < v_{th}$ gives, as a lower limit, the *ordinary opacity sampling;* and for sufficiently high velocities ($\Delta v > v_{th}$) the integration over a radius interval represents the *Sobolev optical depth* ($\Delta\tau$) of a local resonance zone (cf. Sellmaier 1996; Pauldrach et al. 1997). Note that at sufficiently high velocities all lines are included in the radiative transfer if the sampling grid is fine enough. Hence, in this case, the *'opacity sampling method'* becomes an *exact solution.*

First results obtained with this procedure have already been published. Sellmaier et al. (1996) showed that their non-LTE line-blocked O-star wind models solve the long-standing He III problem of H II regions for the first time. Pauldrach et al. (1996) applied their non-LTE models, based on a slightly different

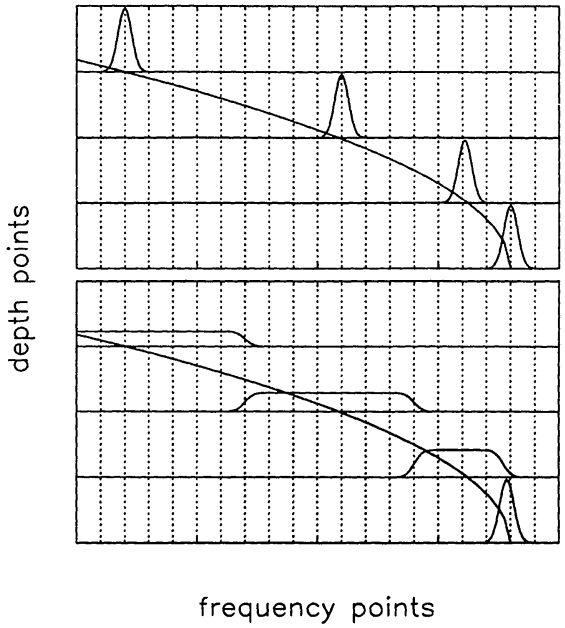

Figure 4. *Upper panel:* the line profile is simply shifted along $\nu_{\rm CMF}$, represented by the curve. *Lower panel:* a boxcar profile is assumed for each depth point.

blocking procedure, to SNIa, and Hummel et al. (1997) carried out non-LTE line-blocked models for classical novae.

3.3. The Treatment of Line Blanketing

The effect of line absorption and emission on the temperature structure is usually referred to as *line blanketing.* Although the processes involved are complex, they always increase the Rosseland optical depth ($\tau_{\rm Ross}$). In deeper layers ($\tau_{\rm Ross} > 0.1$), where true absorptive processes dominate, this leads directly to an enhancement of the temperature, since in this part the temperature is primarily determined by $\tau_{\rm Ross}$.

Thus, if we neglect the influence of the metals in a first step, the temperature structure can be easily calculated using the concept of *non-LTE Hopf functions* (cf. Santolaya-Rey et al. 1997). These functions are based on a parameterization of the temperature stratification obtained from radiative-equilibrium calculations of hydrostatic, plane-parallel H and He non-LTE models, and have been adapted to the spherical case. Fig. 5 shows for an O-dwarf model (henceforth O40; $T_{\rm eff} = 40\,000$ K), that this method leads to almost identical results for the temperature structures obtained by two completely independent codes. The reliability of this method is further proven by the resulting flux conservation which, as shown on the lower panel of Fig. 5, is on the 1% level. Below we will show that the method can also be extended in order to account for the influence of spectral lines (i.e., line blanketing).

In the outer part of the expanding atmosphere ($\tau_{\rm Ross} < 0.1$), where scattering processes start to dominate, the effect of line absorption and emission

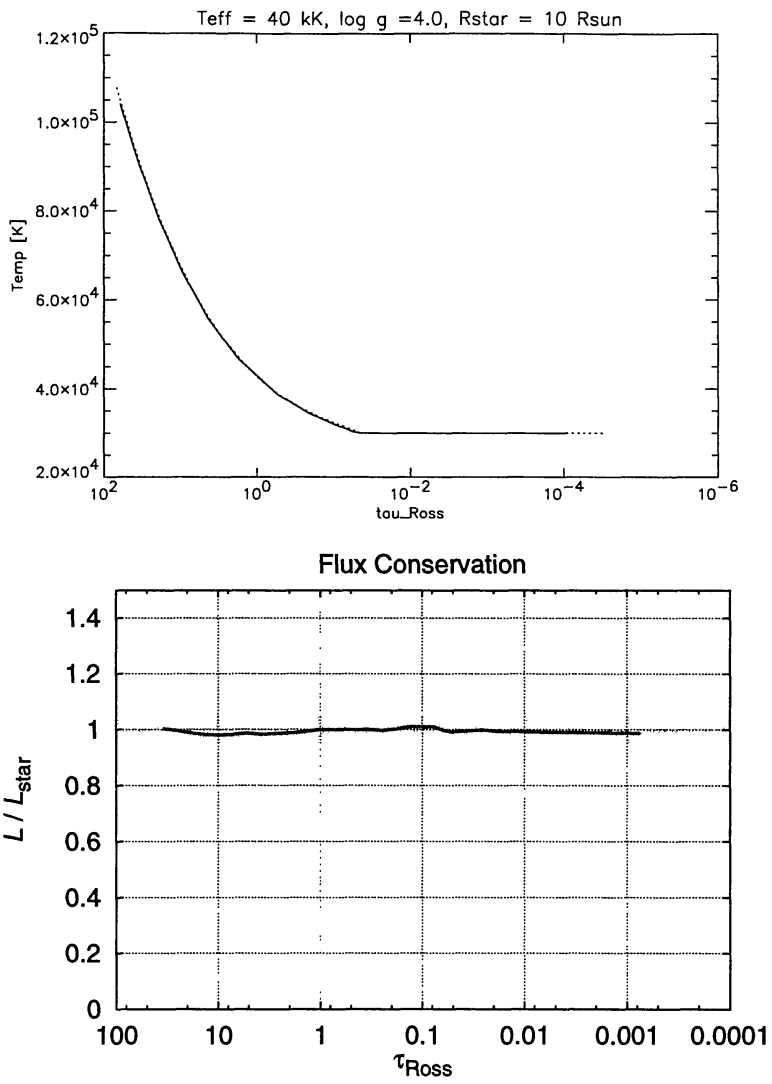

Figure 5. Temperature structure for a pure H/He O40 model without blanketing. *Upper panel:* comparison of temperature structures – our model, fully drawn; Puls et al. (1998), dotted. Lower panel: flux conservation (shown is the calculated luminosity divided by the conserved value) for our model.

on the temperature structure is more difficult to treat. In principle, there are two possibilities: either one calculates for radiative equilibrium, or for balanced heating and cooling rates where all processes have to be included – bound-free, free-free, and collisions. As the $\tau_{\rm Ross}$ values are small in this part, and hence most frequency ranges are optically thin, the latter method turned out to be more suitable.

In order to get an impression of the influence of the blanketing effect, we performed a first simulation for the O40 model where line blocking, but not blanketing, was treated (i.e., we fixed the non-LTE Hopf function).

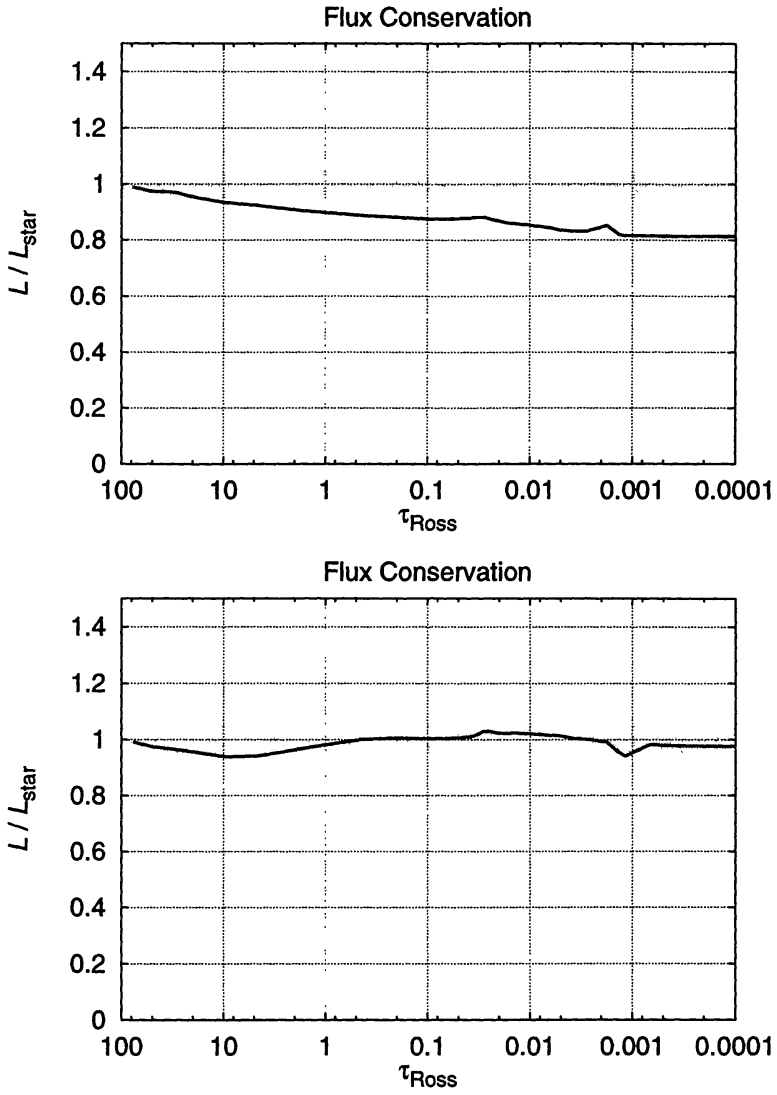

Figure 6. Flux conservation for an O40 model. *Upper panel:* blocking effects, but not blanketing effects, are included; *Lower panel:* both effects are treated consistently.

As displayed in Fig. 6, we found a flux deviation which already starts in the inner part, $\tau_{\rm Ross} < 50$, and reaches a value of 15% at $\tau_{\rm Ross} = 0.1$. (We note that this is not the worst case; for some supergiant models we obtained flux deviations of up to 50%.) This clearly shows the importance of blanketing effects and the need to correctly account for them. Moreover, from these calculations it turns out that absorptive line opacities dominate the total opacity down to an optical depth of $\tau_{\rm Ross} > 0.1$ (see also below – Fig. 8). This result is somewhat in contradiction to Schaerer & Schmutz (1994), who found the dominance of scattering opacities over absorptive opacities even at these depths. However, their finding is misleading since their absorptive opacities include only continuum absorption, whereas true line absorption processes are neglected.

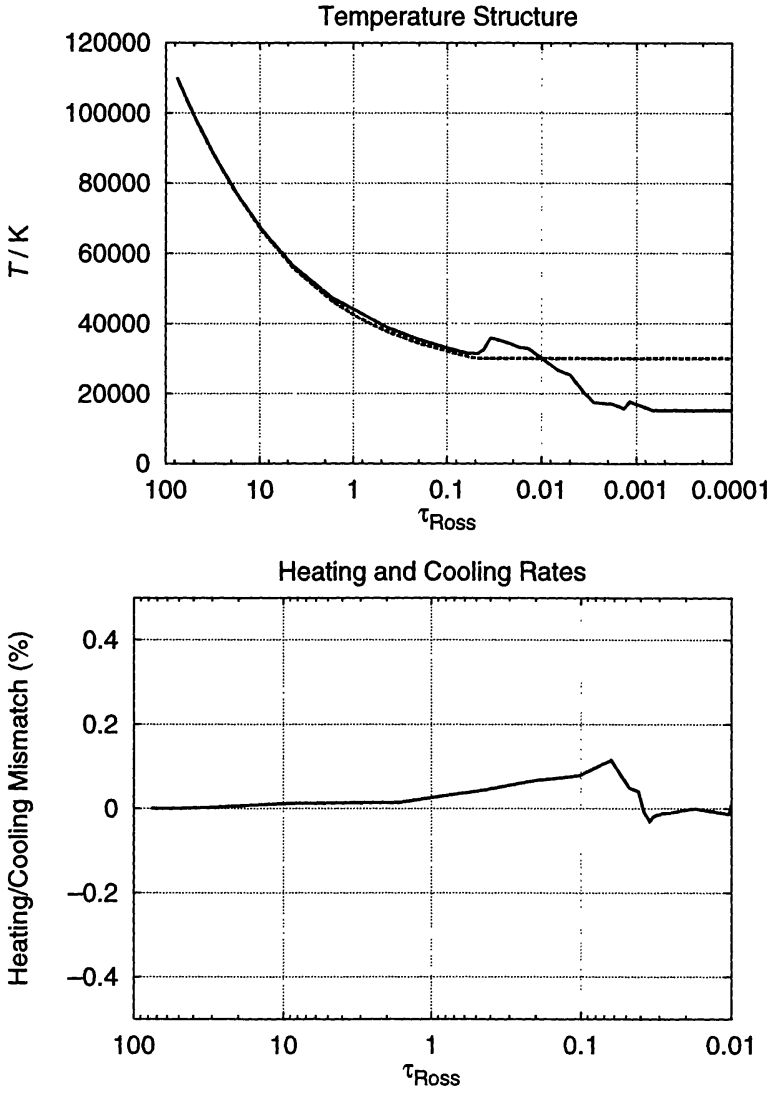

Figure 7. *Upper panel:* temperature structure for the final O40 model where blocking and blanketing effects are included; *Lower panel:* mismatch of the heating and cooling rates for the same model.

In a next step, *line blocking* was treated *consistently.* Using the method of the *non-LTE Hopf functions* this is an easy task, since we just have to update the parameters involved by a flux-correction procedure applied at different values of the optical-depth scale (cf. Pauldrach et al. 1997). As can be inferred from Fig. 6 the flux is conserved again for this model with an accuracy of a few per cent.

Figure 7 displays the resulting temperature structure and shows that the temperature increases by 2000 K at $\tau_{\rm Ross} = 1$. Also shown is the mismatch of the heating and cooling rates, which immediately goes to zero in the outer part ($\tau_{\rm Ross} < 0.07$) where it is applied for correcting the temperature structure. This

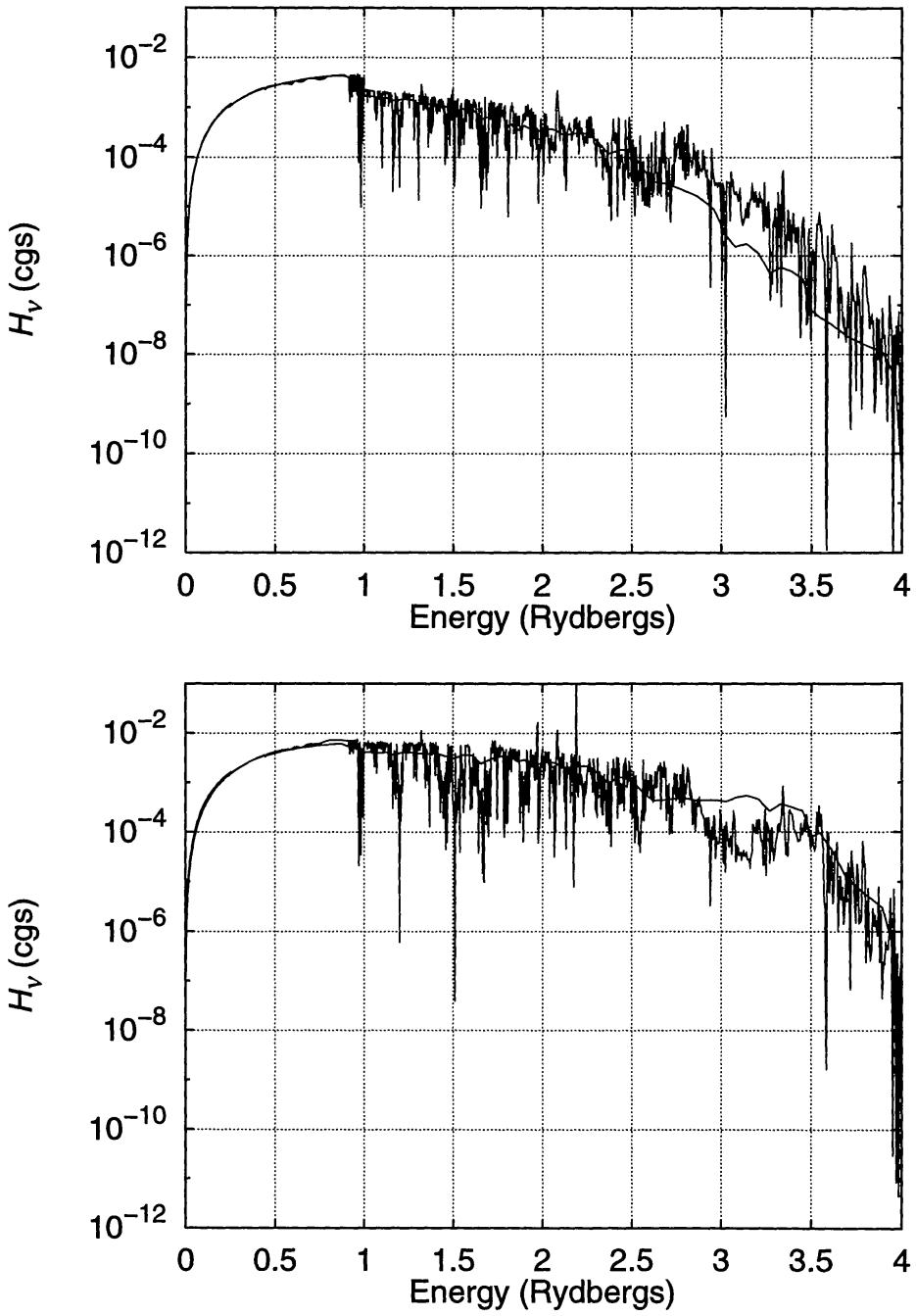

Figure 8. Comparison of EUV spectra from our models and plane-parallel LTE models of Kurucz. The upper panel shows the spectrum of our final O40 dwarf model ($T_{\rm eff} = 40\,000\,{\rm K}, \log g = 4.0$) and the emergent fluxes from Kurucz ($T_{\rm eff} = 40\,000\,{\rm K}, \log g = 4.5$). The lower panel shows the spectrum of our O50 supergiant model ($T_{\rm eff} = 50\,000\,{\rm K}, \log g = 3.8$) and the emergent fluxes from Kurucz ($T_{\rm eff} = 50\,000\,{\rm K}, \log g = 5.0$).

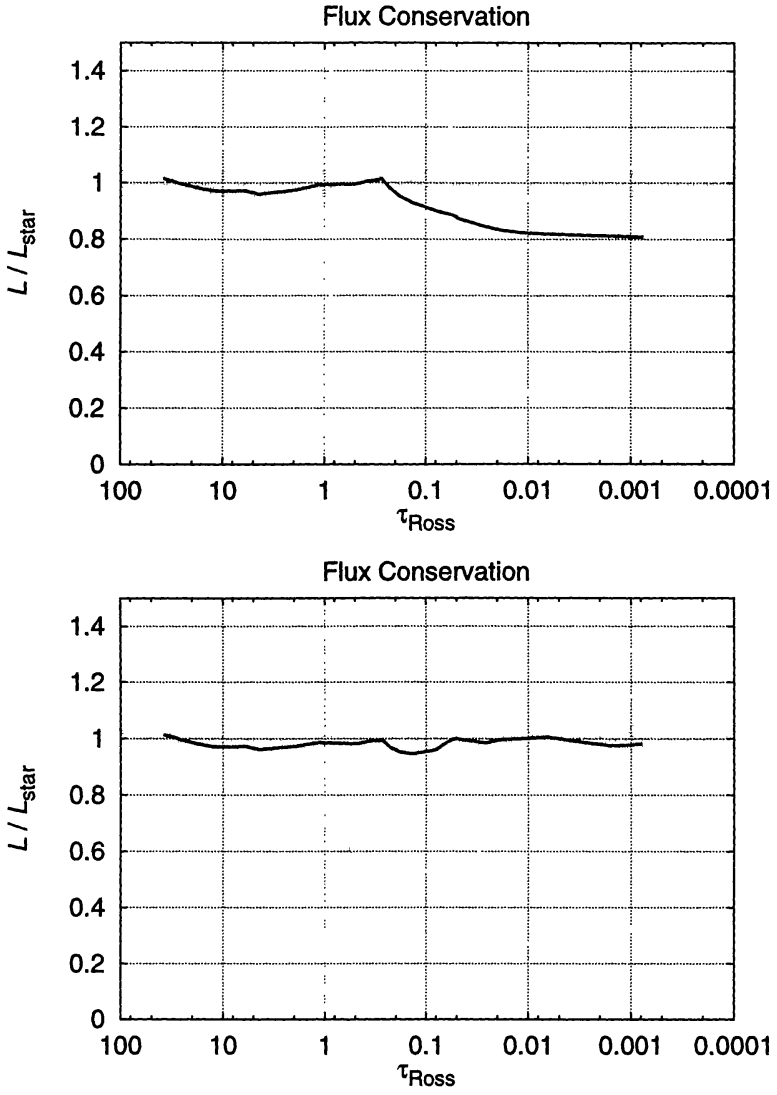

Figure 9. Flux conservation for an O50 model. *Upper panel:* not corrected for self-shadowing; *Lower panel:* corrected for self-shadowing.

produces the pronounced hump and the successive decrease of the temperature in this part.

In Fig. 8 we compare our calculated EUV blocking spectrum with the emergent fluxes from an appropriate Kurucz (1992) model which is based on LTE and plane-parallel static atmospheres. An important point shown is that we obtain almost the same blanketing effect as Kurucz. This is inferred from the redward side of the H edge where the curves are nearly identical, and thus the temperature has to rise in the continuum-forming region in the same way for both models. As absorptive opacities necessarily dominate in LTE, this result requires the same for our model at least for optical depths larger than 0.1. We have already mentioned this finding above. Another important feature observed in Fig. 8 is that the line blocking is less pronounced for our model above 2.7 Ryd;

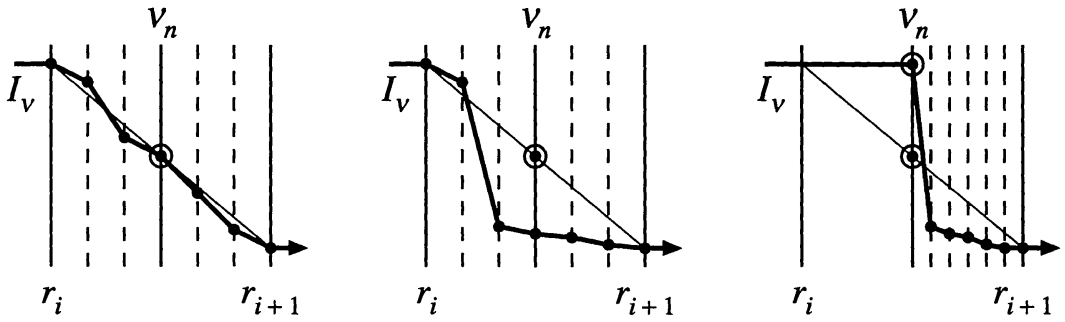

Figure 10. Schematic sketch to illustrate the problem of *self-shadowing* (symbols are explained in the text).

hence we obtain more flux in this frequency range. The opposite result, however, was found for a supergiant model with an effective temperature of $T_{\rm eff} = 50\,000$ K (henceforth O50). As is shown in Fig. 8 (lower panel), less flux appears for our model above 2.7 Ryd, and the blanketing effect is also slightly less pronounced. We attribute the latter result to the influence of the strong wind (mass-loss rate of $\dot{M} = 12 \times 10^{-6}\, M_\odot/{\rm yr}$) on the density structure, which is very different from the static case.

The most surprising result observed so far for our O50 model is the strong absorption features which originate in the outer, and hence scattering, part of the wind. As these features are not balanced by corresponding emission features (in a pure scattering atmosphere this has to be the case in order to conserve the energy), and as this hot star emits most of its flux in the EUV blocking part, we should observe a considerable flux deviation.

Figure 9 (upper panel) shows that this is indeed the case – flux is not conserved by up to 20% in the scattering-dominated part of the wind. This is the result of an inconsistency which became evident for the O50 model, because of the strong wind which favours the influence of scattering lines on the emergent EUV spectrum in the outer part of the atmosphere. The reason for this inconsistency is *self-shadowing* – i.e., the interaction of strong wind lines with themselves. It occurs because the incident intensity used to calculate the bound-bound transition rates for any arbitrary line is already affected by that particular line itself, since the line has already been treated for line blocking in the iteration cycle. We refer to the schematic sketch above (Fig. 10) to illustrate this point.

In a given velocity interval, between successive radial depths points, $r_i \rightarrow r_{i+1}$, we need to estimate the intensity I_ν (indicated in the Figure by dots) seen by lines (indicated by dashes) contained in the equivalent frequency interval. In general, we use the intensity I_{ν_n} (indicated by $\odot$) calculated at the sampling point (indicated by ν_n), which represents a fair mean value for the *true incident radiation* of the individual lines in this interval, provided all the lines are of similar strength (see left panel of Fig. 10).

However, if there is a dominating line in the interval (middle panel of Fig. 10), the intensity taken at the sampling point (and used for the bound-

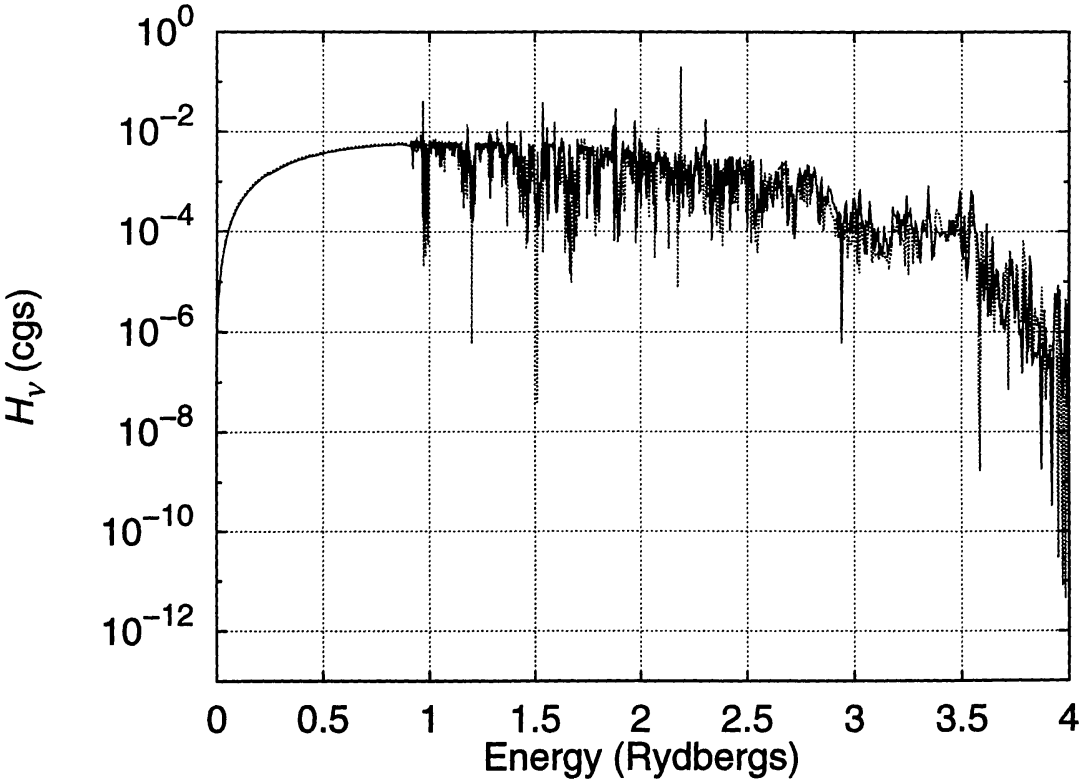

Figure 11. Comparison of EUV spectra from our O50 supergiant model ($T_{\rm eff} = 50\,000\,{\rm K}, \log g = 3.8$) with (fully drawn) and without (dotted) corrections for self-shadowing.

bound transitions belonging to lines in this interval) is much smaller than the *true incident radiation* for this line, because the line has already influenced this value considerably. This is what we mean by *self-shadowing*. The consequence is that the source function of this line is underestimated; thus, the scattering processes are not correctly described, and, hence, energy is not conserved. The solution, however, is quite simple. For calculating the bound-bound rates – having identified the dominating lines – we just irradiate them by an incident intensity which is independent of the lines in the considered interval (right panel of Fig. 10). With this correction the flux is again conserved, as shown in Fig. 9 (lower panel).

A comparison of the EUV blocking spectra calculated with and without this correction procedure (see Fig. 11) shows that the strong absorption features vanished, and the smaller ones are now compensated by corresponding emission features.

4. Summary and Future Work

We have presented the status of our hydrodynamic non-LTE models for expanding atmospheres, where accurate atomic data, the EUV and X-ray radiation from

shock-heated matter, and a consistent calculation of line blocking and blanketing are treated.

That this effort is worthwhile has already been demonstrated by the quantitative spectroscopic analyses of seven O stars. Nevertheless, we still have to show that the realistic models from our improved method also lead to improvements in detailed spectrum synthesis, or whether refinements to the method are still required. In addition, we need to establish whether the discrepancies between observed and theoretically predicted wind-momentum rates, which appear to exist for O stars (cf. Puls et al. 1996), can be removed by means of our new models. Furthermore, we still have to investigate the impact of our new ionizing fluxes on the quantitative analysis of emission-line spectra of H II regions and planetary nebulae.

Acknowledgments. This research was supported by the DFG in the 'Gerhard Hess Programm' under grant Pa 477/1-3.

References

Castor, J. I., Abbott, D. C., Klein, R. I., 1975, ApJ, 195, 157

Cunto, W., Mendoza, C., 1992, Rev. Mex. A&A, 23, 107

Eissner, W., Jones, M., Nussbaumer, H., 1974, Computer Physics Comm., 8, 270

Feldmeier, A., 1995, A&A, 299, 523

Feldmeier, A., Kudritzki, R.-P., Palsa, R., Pauldrach, A. W. A., Puls, J., 1997, A&A, 320, 899

Feldmeier, A., Pauldrach, A., Puls, J., 1998 in Boulder-Munich II: Properties of Hot, Luminous Stars (ASP Conf. Series, Vol. 131), ed. I. D. Howarth (ASP, San Francisco), p. 278

Haser, S. M., Pauldrach, A. W. A., Lennon, D. J., et al., 1997, A&A, in press

Hillier, D. J., Miller, D. L., 1997, A&A, in press

Hubeny,I., Heap, S. R., Lanz, T., 1998, in Boulder-Munich II: Properties of Hot, Luminous Stars (ASP Conf. Series, Vol. 131), ed. I. D. Howarth (ASP, San Francisco), p. 108

Hummel, W., Pauldrach, A. W. A., Williams, R., Lennon, M., Kudritzki, R.-P., 1997, in 13th North American Workshop on Cataclysmic Variables (ASP Conf. Series), eds. S. Howell, E. Kuulkers & C. Woodward (ASP, San Francisco), in press

Hummer, D. G., Rybicki, G. B., 1985, ApJ, 293, 258

Hummer, D. G., Berrington, K. A., Eissner, W., Pradhan, Anil K., Saraph, H. E., Tully, J. A., 1993, A&A, 279, 298

Hunsinger, J., 1993, Diplomarbeit, Universitätssternwarte München

Kudritzki, R. P., 1998, in Stellar Astrophysics for the Local Group (Proceedings of the VIII Canary Islands Winter School), eds. A. Aparicio, A. Herrero & F. Sanchez (Cambridge University Press), p. 147

Kurucz, R. L., 1979, ApJS, 40, 1

Kurucz, R. L., 1992, Rev. Mex. A&A, 23, 45

Lucy, L. B., Solomon, P., 1970, ApJ, 159, 879

Morton, D. C., Underhill, A. B., 1977, ApJS, 33, 83

Nussbaumer, H., Storey, P. J., 1978, A&A, 64, 139

Owocki, S. P., Castor, J. I., Rybicki, G. B., 1988, ApJ, 335, 914

Pauldrach, A. W. A., Kudritzki, R.-P., Puls, J., Butler, K., Hunsinger, J., 1994a, A&A, 283, 525

Pauldrach, A. W. A., Feldmeier, A., Puls, J., Kudritzki, R. P., 1994b, Space Sci. Rev., 66, 105

Pauldrach, A. W. A., Duschinger, M., Mazzali, P. A., Puls, J., Lennon, M., Miller, D. L., 1996, A&A, 312, 525

Pauldrach, A. W. A., et al., 1997, in preparation

Peytremann, E., 1974, A&A, 33, 203

Prinja, R. K., Howarth, I. D., 1986, ApJS, 61, 867

Puls, J., 1987, A&A, 184, 227

Puls, J., Hummer, D. G., 1988, A&A, 191, 87

Puls, J., Kudritzki, R.-P., Herrero, A., Paudrach, A. W. A., Haser, S. M., Lennon, D. J., Gabler, R., Voels, S. A., Vilchez, J. M., Wachter, S., Feldmeier, A., 1996, A&A, 305, 171

Puls, J., Kudritzki, R.-P., Santolaya-Rey, A. E., Herrero, A., Owocki, S. P., McCarthy, J. K., 1998, in Boulder-Munich II: Properties of Hot, Luminous Stars (ASP Conf. Series, Vol. 131), ed. I. D. Howarth (ASP, San Francisco), p. 245

Raymond, J. C., Smith, B. W., 1977, ApJS, 35, 419

Santolaya-Rey, A. E., Puls, J., Herrero, A., 1997, A&A, 323, 488

Schaerer, D., Schmutz, W., 1994, A&A, 288, 231

Schaerer, D., de Koter, A., 1997, A&A, 322, 598

Seaton, M. J., Yan Yu, Mihalas, D., Pradhan, Anil K., 1994, MNRAS, 266, 805

Sellmaier, F., Yamamoto, T., Pauldrach, A. W. A., Rubin, R. H., 1996, A&A, 305, L37

Sellmaier, F., 1996, Doctoral Thesis, Universitätssternwarte München

Sneden, C., Johnson, H. R., Krupp, B. M., 1976, ApJ, 204, 281

Taresch, G., Kudritzki, R. P., Hurwitz, M., et al., 1997, A&A, 321, 531

Walborn, N. R., Nichols-Bohlin, J., Panek, R. J., 1985, IUE Atlas of O-Type Spectra from 1200 to 1900Å (NASA RP-1155)

Discussion

Gies: What difference does line-blanketing make to the effective temperature you would estimate for a given stars?

Pauldrach: It depends whether you have a dwarf or a supergiant; in the case of a 50 kK supergiant it's up to 50% in the flux, which I would say corresponds to 4–5 kK.

Gies: How does this relate to the wind blanketing discussed by Abbott & Hummer?

Pauldrach: The effect I showed is due to both wind blanketing, and photospheric line blanketing. The dominant influence is, however, due to true line-absorption processes acting in the photospheric region and the lower part of the wind, at velocities comparable to the sound velocity.

Crowther: Your models seem to be in line with the Kurucz model distributions in terms of ionizing fluxes for the very hot O stars, whereas I thought Daniel Schaerer and Alex de Koter got quite large differences?

Pauldrach: With regard to my previous answer, I think this is the case for the integrals of the ionizing fluxes of at least the O dwarf models. Concerning the differences found by Schaerer and de Koter, I think the authors should get the chance to explain that...

Schaerer: I will discuss this when I give my talk tomorrow [p. 310].

Kudritzki: Could you say something about the effect of shocks in the wind?

Pauldrach: Yes, we include the radiative emission by shock-heated matter but I didn't have time to discuss this. For the treatment of the corresponding emission coefficient we use an approximate description, using a filling factor and a cooling function – calculated with the Raymond & Smith (1977) code – for the shock emission. Due to this procedure we have two free parameters: a filling factor (which is fixed by a comparison of the observed and calculated X-ray luminosity, where the first value is obtained from Rosat observations), and the jump velocity, which determines the immediate post-shock temperature and hence the cooling function. For the jump velocity we found a proportionality to the local velocity in units of the terminal velocity, and the turbulent velocity. As an example, we have shown that our model for ζ Pup fits the ROSAT observation very well.